

Equation of state and phonon frequency calculations of diamond at high pressures.

K. Kunc,* I. Loa, and K. Syassen†

Max-Planck-Institut für Festkörperforschung, Heisenbergstrasse 1, D-70569 Stuttgart, Germany

(Dated: 29 April 2003)

The pressure-volume relationship and the zone-center optical phonon frequency of cubic diamond at pressures up to 600 GPa have been calculated based on Density Functional Theory within the Local Density Approximation and the Generalized Gradient Approximation. Three different approaches, viz. a pseudopotential method applied in the basis of plane waves, an all-electron method relying on Augmented Plane Waves plus Local Orbitals, and an intermediate approach implemented in the basis of Projector Augmented Waves have been used. All these methods and approximations yield consistent results for the pressure derivative of the bulk modulus and the volume dependence of the mode Grüneisen parameter of diamond. The results are at variance with recent precise measurements up to 140 GPa. Possible implications for the experimental pressure determination based on the ruby luminescence method are discussed.

PACS numbers: PACS: 71.15.Nc, 63.20.-e, 62.50.+p

I. INTRODUCTION

Diamond is the archetype of the covalently bonded, tetrahedrally coordinated insulators. Its extreme hardness is highly valued in technology and is also exploited in high pressure research when using the diamond anvil cell. The elastic properties of diamond near ambient conditions are well characterized through ultrasonic and Brillouin techniques. However, as a consequence of the small compressibility, the changes in elastic properties under high hydrostatic pressure are not well confined experimentally. This, for instance, applies to the variation of the bulk modulus B with pressure P , $B'_0 = (dB/dP)_{P=0}$, a basic parameter in the equation-of-state (EOS) modelling. A property closely related to the compression behavior of diamond is the pressure-induced frequency shift of the threefold degenerate F_{2g} zone-center optical phonon mode; its shift with pressure provides an approximate measure of the change in relative density, because the mode Grüneisen parameter is close to one.^{1,2,3,4}

High-pressure x-ray diffraction experiments^{5,6,7} yield the ambient-pressure bulk modulus B_0 in good agreement with acoustic measurements.^{8,9,10,11,12} The analysis of diffraction data is usually based on adopting $B'_0 = 4.0$ obtained from ultrasonic measurements up to 0.2 GPa.⁸ The only exception is the recent diffraction study of diamond to 140 GPa by Occelli *et al.*,⁷ who report $B'_0 = 3.0$, at variance with the ultrasonic measurement. It was subsequently argued¹³ that the ruby pressure calibration¹⁴ employed in the diffraction work of Ref. [7] may need a revision. If so, the pressure shift of the F_{2g} phonon frequency, also studied by Occelli *et al.* up to 140 GPa, should be affected in a similar manner. The F_{2g} phonon mode behavior at high pressures was frequently studied by Raman spectroscopy^{1,2,3,4,5,15,16,17,18,19,20} and its possible role in pressure calibration was addressed early on.^{4,5,21}

We report the calculation of the EOS and optical phonon frequency of diamond at high pressures within Density Functional Theory (DFT). Extensive theoretical

work on diamond under pressure by *ab initio* methods has addressed changes in bonding, elasticity, lattice dynamics, thermodynamical properties, phase stability, and electronic excitations, see, e.g., Refs. [4,22,23,24,25,26,27,28,29,30,31,32,33,34,35,36,37,38,39,40,41,42]. Here, we are interested in a specific question: What are, based on different implementations and approximations of DFT, the constraints on B'_0 of diamond and on the nonlinear pressure shift of the optical phonon frequency. The calculated values of B'_0 reported in the literature scatter by about 25%, spanning a range similar to that of the experimental results. Calculated pressure effects on the optical phonon frequency were reported in Refs. [4] and [27]. Results of a more recent calculation⁴¹ show some disagreement with Refs. [4] and [27]. In view of new experimental results⁷ and the – at least apparent – uncertainties in the previous theoretical predictions we considered it worthwhile to revisit the calculation of the EOS and optical phonon frequency of diamond under pressure, combined with accurate procedures to extract the parameters of interest.

II. DETAILS OF THE CALCULATIONS

The total energy calculations performed in this work are based on DFT⁴³ within, on one hand, the Local Density Approximation⁴⁴ (LDA) and, on the other hand, the Generalized Gradient Approximation^{45,46} (GGA). In order to grasp the uncertainties consequent to the choice of the computational method and of its inherent assumptions, we are using simultaneously three different approaches, viz. the pseudopotential method applied in the basis of plane waves^{47,48,49,50} (PW), an all-electron method relying on the Augmented Plane Waves plus Local Orbitals^{51,52,53} (APW+lo), and an intermediate approach implemented in the basis of Projector Augmented Waves^{54,55} (PAW); the latter approach⁵⁶ treats the valence states as part of an all-electron problem and describes them by all-electron wave-functions.

The pseudopotential employed is the “dual-space” separable pseudopotential of Hartwigsen, Goedecker, and Hutter⁵⁷ and its GGA counterpart constructed by X. Gonze^{47,58}; the PAW potentials were constructed by G. Kresse and denoted as C_h in Ref. [54]. All methods take into account scalar-relativistic corrections (though no meaningful contribution expected in diamond), either explicitly (APW+lo) or through the construction of the (pseudo-)potentials.

The numerical convergence of all three methods, with respect to the size of the basis set and k-space sampling was thoroughly tested. The plane-wave cutoffs of 75 Hartree and 1500 eV were applied with, respectively, the PW and the PAW-basis. These rather large values are required for getting reliable results for the *pressure* which is calculated analytically, in both approaches, with the aid of the stress theorem.^{59,60} In the APW+lo method a muffin-tin radius of $R_{MT} = 1.2$ a.u. was used. The plane-wave expansion was limited by $R_{MT} \times K_{max} = 9$ and the charge density Fourier expansion by $G_{max} = 20$ Ry^{1/2}. In the APW+lo method the $P(V)$ results were generated from $E^{\text{tot}}(V)$ fitted as described below.

The integration over the Brillouin zone is performed using the same set of 28 k-points in the irreducible wedge in both plane-wave based approaches; the set was generated by the “special points” approach⁶¹ using a $6 \times 6 \times 6$ mesh with 4 different fractional shifts. In the APW+lo approach the tetrahedron integration was employed,^{62,63} based on a uniform, Γ -centered $10 \times 10 \times 10$ mesh of 47 k-points.

The frozen-phonon approach, which consists in the evaluation of the total energy E^{tot} of the crystal with frozen-in atomic displacements, was applied (in the two plane-wave based methods only) with the same cutoffs and with the same k-point mesh ($6 \times 6 \times 6 + 4$ shifts) which, due to the lowered symmetry, results in a 91 k-points set. Small displacements $\vec{u}(1) = \pm(u, u, u)$ and $\vec{u}(2) = \mp(u, u, u)$ with $u/a = 0.002$ were applied to the two atoms of the basis – thus either compressing or stretching the C(1) – C(2) bond, like in the zone-center F_{2g} mode – and the two values obtained for ΔE^{tot} [viz. the ΔE^{tot} (outward) and ΔE^{tot} (inward)] were averaged. The eigenfrequency is then found from the expression for the energy of a harmonic oscillator

$$\Delta E^{\text{tot}} = \frac{1}{2} M \omega^2 [|\vec{u}(1)|^2 + |\vec{u}(2)|^2] , \quad (1)$$

where M is the atomic mass. The above-mentioned averaging procedure of the ΔE^{tot} (outward) and ΔE^{tot} (inward) eliminates the cubic contribution to ΔE^{tot} . It turns out that the remaining quartic anharmonicity is small at $u/a = 0.002$ and contributes to the uncertainty of the resulting eigenfrequencies by less than 0.1 cm⁻¹ (checked by repeating the same calculations with displacements $u/a=0.0015$ and 0.003).

Total energies, pressures, and phonon frequencies were calculated at 12 different volumes ranging from 6.35 Å³/atom down to 3.35 Å³/atom, i.e., for about 10%

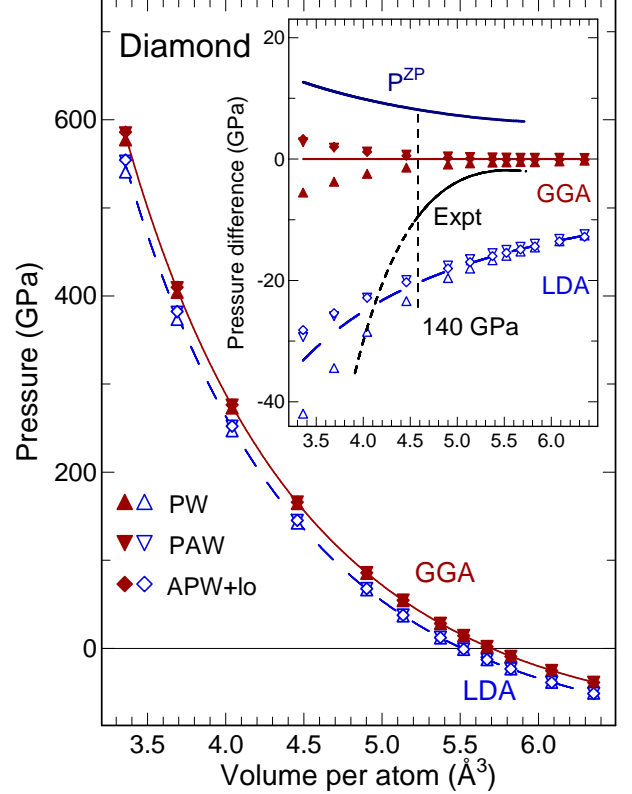


FIG. 1: Pressure-volume results for diamond from plane wave (PW, triangles up), projector augmented wave (PAW, triangles down), and all-electron (APW+lo, diamonds) calculations. Solid and dashed lines represent fits of Eq. 2 to the combined GGA (filled symbols) and LDA (open symbols) results, respectively. The inset offers a zoomed view of pressure differences relative to the average $P(V)$ relation for GGA calculations, including the differences for experimental data of Ref. [7] and their extrapolation. The volume dependence of the zero-point pressure $P^{ZP}(V)$ is also shown in the inset.

volume expansion to 40% compression relative to the experimental equilibrium volume of 5.6725 Å³/atom at 300 K.⁶⁴ The lower volume limit corresponds to roughly 600 GPa maximum pressure.

III. PRESSURE-VOLUME RELATIONSHIP

A. Analytical form

Figure 1 shows calculated pressures as a function of volume. An excellent consistency of the data points obtained by the three different methods is immediately apparent. Also, the present results substantiate the claims made in Ref. [55] concerning the equivalence of the PAW approach with all-electron methods such as that of Ref. [51].

The proper analysis of the $P(V)$ results yields the equilibrium properties V_0 , $B_0 = -V_0(dP/dV)_0$, and $B'_0 = (dB/dP)_0 = (d \ln B / d \ln V)_0$ (throughout this

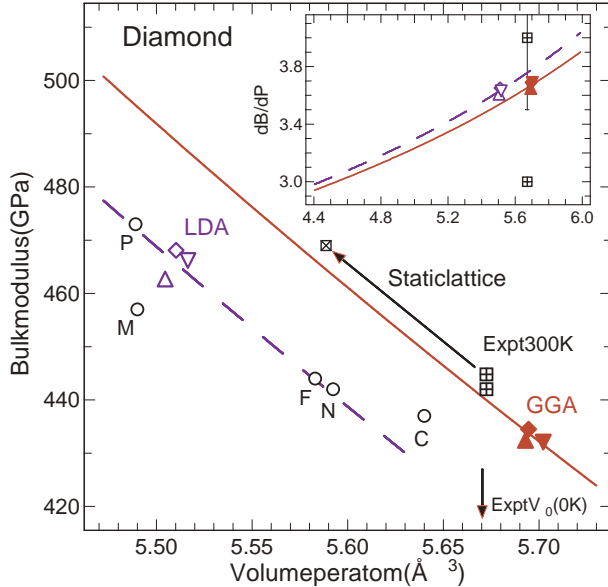


FIG. 2: Bulk modulus B_0 of diamond obtained from different calculations plotted against the calculated equilibrium volume V_0 . Symbols for the present GGA and LDA results as in Fig. 1. Other calculated values of B_0 [24,27,29,33,35] are indicated by open circles (the attached letters refer to the first-author name). The experimental values of B_0 originate from ultrasonic measurements⁸ and Brillouin scattering.¹¹ The solid (dashed) line refers to the volume dependence of the bulk modulus for combined GGA (LDA) results. The inset shows the pressure derivative of the bulk modulus versus atomic volume. The calculated B'_0 values and the two experimental ones are represented by symbols.

manuscript the subscript 'zero' refers to zero (ambient) pressure or equilibrium volume, either calculated or experimental depending on context). One also needs to identify an analytical form of the $P(V)$ behavior which, using the above parameters, fits the calculated pressures over the full volume range.

We have tried several of the common equation-of-state forms.^{65,66,67,68} The best analytical expression, in the least-squares sense, was identified as

$$P(V) = 3B_0X^{-n}(1-X)\exp[\eta(1-X)] \quad (2)$$

where $X = (V/V_0)^{1/3}$, $\eta = 3B'_0/2 + 1/2 - n$, and $n = 7/2$. With $n = 7/2$ Eq. 2 is a blend of the Vinet⁶⁷ (or Rydberg)^{69,70} form and the Holzapfel⁶⁸ expression, for which $n = 2$ and $n = 5$, respectively. Actually, the parameter n varies between 3.4 and 3.6 for individual sets of calculated $P(V)$ data of diamond. Without loss of significant digits in the fitted parameters of interest, we fix n at a value of 7/2; in this case the energy versus volume relation, obtained by integration of Eq. 2, can be written without invoking special functions other than the error function:

$$E(V) = E_0 + 9B_0V_0[f(V) - f(V_0)]\exp(\eta)/\sqrt{\eta} \quad (3)$$

$$f(V) = \sqrt{\eta}(2\eta + 1)\text{erf}(\sqrt{\eta}X^2) + 2\sqrt{\eta}\exp(-\eta X)/X^2.$$

Here, E_0 is the energy at $V = V_0$. Equation 2 was used to fit the $P(V)$ results obtained via the stress theorem (PW and PAW methods), while Eq. 3 served to determine the EOS parameters from total energies (APW+lo method). For the PW and PAW methods it was carefully checked that the directly calculated $P(V)$ data are consistent with those obtained by differentiation of $E(V)$. For all sets of calculated $P(V)$ or $E(V)$ data the rms deviations were less than 0.04 GPa or 0.05 meV, respectively.

Aleksandrov *et al.*⁵ pointed out that a quadratic dependence of pressure on change in relative density $\Delta\rho/\rho_0 = V_0/V - 1$, written as

$$P(\rho) = B_0 \frac{\Delta\rho}{\rho_0} \left[1 + \frac{B'_0 - 1}{2} \frac{\Delta\rho}{\rho_0} \right], \quad (4)$$

applies in the case of diamond for $P \leq 100$ GPa. This expression is found to fit the calculated results up to 600 GPa quite well. It is only in the statistical sense that Eq. 4 is slightly inferior to Eq. 2, i.e., the rms deviations are larger by a factor of two, but this is not relevant for the present discussion. The bulk modulus, obtained by differentiation of Eq. 4 with respect to normalized volume, is given by

$$B(\rho) = B_0 \frac{\rho}{\rho_0} \left[1 + (B'_0 - 1) \frac{\Delta\rho}{\rho_0} \right]. \quad (5)$$

Equation 5 corresponds to a quadratic dependence of the bulk modulus on relative change in density.

B. Calculated EOS parameters

The obtained pairs of (V_0, B_0) values are displayed in Fig. 2. Within a given approximation for the exchange-correlation functional (GGA or LDA), the three methods employed here (PW, PAW, APW+lo) yield results for V_0 and B_0 which are in very good agreement with each other. The choice of the exchange-correlation functional, however, leads to differences of 4% in V_0 and 5% in B_0 , reflecting in part the well-known overbinding of the LDA. All B'_0 values (cf. inset to Fig. 2) fall into a narrow range between 3.6 and 3.7, the difference between averaged LDA and GGA results being close to 1%.

Since the calculated EOS parameters clearly split into two groups, i.e. the GGA and LDA results, with nearly identical parameter values within each group, we have combined the $P(V)$ points for GGA and LDA, respectively, to obtain the GGA and LDA parameters V_0 , B_0 , and B'_0 listed in Table I. The corresponding $P(V)$ relations are shown by solid and broken lines in Fig. 1, where the inset illustrates deviations of individual calculated results from the average curves. Similarly, the solid and broken lines in Fig. 2 and its inset show the corresponding volume dependences of the bulk modulus and its pressure derivative.

TABLE I: Calculated equation-of-state [Eq. 2] and optical phonon parameters of diamond. Selected experimental results are listed in the lower part of the Table. The static-lattice entries correspond to switching off (at $T = 0$ K) the effect of zero point motion. The calculated phonon pressure coefficients are obtained via $(d\omega/dP)_0 = \gamma_0\omega_0/B_0$ with parameters given in the same row of the Table. Likewise, the experimental mode Grüneisen parameters were obtained from the experimental pressure coefficients unless noted otherwise. In the row marked GGA&LDA both the ambient pressure volume and bulk modulus are normalized to one.

Method	V_0 Å ³	B_0 GPa	B'_0	n	ω_0 cm ⁻¹	γ_0	γ'_0	$(d\omega/dP)_0$ cm ⁻¹ /GPa
All LDA	5.510(5)	465(3)	3.63(3)	7/2	1322(2)	1.003(3)	0.79(5)	2.87
All GGA	5.697(4)	433(2)	3.67(3)	7/2	1290(2)	0.995(3)	0.80(5)	3.00
GGA&LDA normalized	1	1	3.65(5)	7/2	1	1.000(5)	0.80(5)	
Expt. $T=300$ K	5.6725 ^a	442 ^b	4.0(5) ^b		1332.5	0.962(15) ^c		2.90(5) ^d
		444.8(8) ^e			1332.40(5) ^e	1.00(3) ^f		3.00(10) ^f
	5.674(1) ^g	446(1) ^g	3.0(1) ^g	2	1333 ^g	$\bar{\gamma}=0.97^g$		2.83 ^g
Expt. $T \rightarrow 0$ K	5.6707 ^a	445 ⁱ			1332.70(3)			
Static lattice	5.5886 ^h	469 ⁱ						
	5.6122 ^j	462 ⁱ						

^aRef. [64].

^bRef. [8]; ultrasonic experiments up to 0.2 GPa.

^cExperimental mode Grüneisen parameters reported in the literature [1,2,3,4,5,15,17,18] vary between 0.90 to 1.06.

^d'Best' value in the literature according to Ref. [20].

^eRef. [11]; Brillouin and Raman scattering.

^fValue obtained for a revised linear pressure coefficient of the ruby line shift as explained in the text.

^gRef. [7]; x-ray diffraction (Vinet fit) and Raman scattering up to 140 GPa. The mode Grüneisen parameter $\bar{\gamma}$ is the average for the pressure range 0–140 GPa.

^hRef. [71]; the classical limit in path integral Monte Carlo simulations.

ⁱEstimated value, see text.

^jRef. [11]; based on extrapolation of isotope effects.

The larger B_0 value for LDA compared to GGA correlates with the smaller equilibrium volume. However, the $B(V)$ curve for LDA falls below that for GGA (see Fig. 2). This also applies to B_0 values obtained in other self-consistent LDA calculations for diamond^{27,29,33,35} (represented by open circles in Fig. 2).

C. Zero-point motion effects

The calculated results for V_0 and B_0 should be compared to experimental properties after 'correction' for vibrational effects. Thermal effects are almost negligible at 300 K because of the high Debye temperature of diamond (~ 2000 K), but zero-point motion needs to be considered. According to Monte Carlo simulations⁷¹ the static-lattice equilibrium volume for diamond is about 5.59 Å³. All the data for V_0 shown in Fig. 2 fall into a range of $\pm 2\%$ around this value. The static-lattice bulk modulus at $V = 5.59$ Å³ is estimated to be 469 GPa (this follows from the experimental values of V_0 and B_0 and the calculated B'_0). Thus, relative to static-lattice properties, the GGA results cannot be considered superior to the LDA ones; they appear better when compared to experimental data because the GGA errors happen to

mimic the zero-point effects.

The zero-point vibrational pressure P^{ZP} , i.e., the isochoric change in pressure when zero-point motion is switched on, is about 6 GPa at the static-lattice value of V_0 .⁷¹ An approximate relation for the volume dependence of P^{ZP} is

$$P^{ZP}(V) \approx -\frac{dP(V)}{dV} \Delta V^{ZP}(V) ,$$

where ΔV^{ZP} is the isobaric volume expansion due to zero-point motion. For getting $\Delta V^{ZP}(V)$ within the quasi-harmonic thermodynamics, we simply refer to the calculated pressure dependence of the zero-point expansion presented in Fig. 10 of Ref. [71]. The corresponding volume dependence of P^{ZP} is displayed in the inset of Fig. 1. P^{ZP} increases by about 6 GPa at 600 GPa. Adding such small changes in P^{ZP} to the calculated $P(V)$ results leads to an increase of the B_0 values by about 1%, but would not affect the calculated B'_0 values (within the estimated uncertainty of the optimum value given below).

D. The essence of the EOS calculations

In Fig. 3, the calculated $P(V)$ relations are plotted in reduced coordinates, i.e. pressure normalized by B_0 ($\Delta\rho/\rho_0$) as a function of $\Delta\rho/\rho_0$. In this representation small differences in ambient-pressure volumes and bulk moduli are suppressed and a linear slope corresponds to a quadratic dependence of pressure on change in relative density (Eq. 4). The LDA and GGA results hardly differ in slope. In this way, Fig. 3 illustrates the main information we extract from our EOS calculations for diamond:

(1) The value of B'_0 does not depend much on crystal potential and basis set issues and on approximations for the exchange-correlation functional. Our average value is

$$B'_0 = 3.65 \pm 0.05,$$

where the small uncertainty reflects the scatter for the different methods of calculation.

(2) Within the volume range considered here, the most appropriate 3-parameter analytical form for the $P(V)$ relation of diamond (Eq. 2 or 4) is transferable between LDA and GGA solutions; only V_0 and B_0 need to be adjusted.

(3) Inserting the calculated B'_0 value and the experimental data for V_0 and B_0 (see Table I) into Eq. 2 (Eq. 4) is considered to yield, on the basis of this work, the optimum representation of the EOS of diamond at 300 K. Actually, at the experimental V_0 the GGA bulk modulus (calculated value of 440 GPa plus 1% correction for zero-point motion effects) happens to be very close to the experimental B_0 , and the calculated pressure at the experimental V_0 is only 2 GPa. Therefore, the optimum EOS corresponds to the $P(V)$ relation obtained from GGA calculations, with only a small correction applied.

E. Comparison with other results for B'_0

Calculated values of B'_0 reported in the literature are 3.54 [24], 3.6, 4.5 [27], 3.24 [29], 3.5 [35] and 3.97 [71]. In some cases, the differences to our result are small. Larger deviations may in part result from the procedure used to extract the EOS parameters (e.g., fit of a Murnaghan equation which is inadequate).

The experimental value $B'_0 = 4 \pm 0.5$ (Ref. [8]) derived from sound speed measurements at low pressures (0.2 GPa) is not sufficiently accurate to test the calculated result.

The only other experimental value of B'_0 stems from the recent x-ray diffraction experiments up to 140 GPa.⁷ The EOS data appear to be of high quality. They were measured using helium as a pressure medium which is considered to provide almost hydrostatic conditions in DAC experiments. The obtained value of $B'_0 = 3.0(1)$ is inconsistent with the ultrasonic result and also significantly smaller than the calculated value. The latter

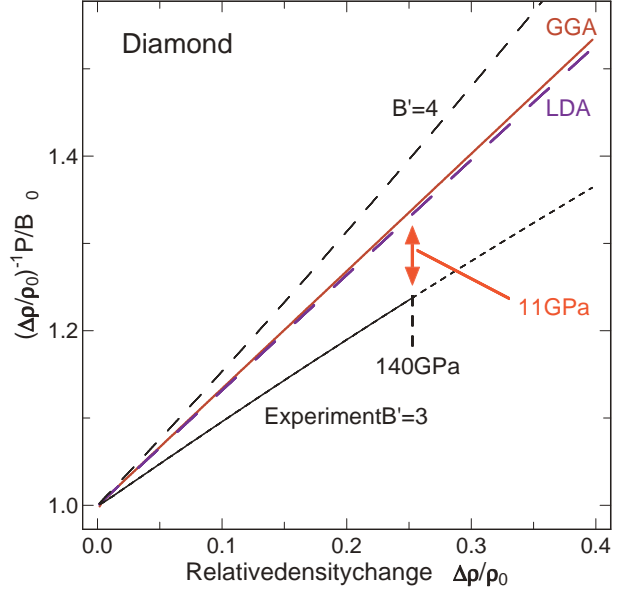


FIG. 3: Calculated pressure-volume relations of diamond in reduced coordinates and using V_0 , B_0 , and B'_0 from Table I. Experimental data of Ref. [7] are shown for comparison. These experiments cover a pressure range of about 140 GPa. The line labelled $B'_0 = 4$ represents the EOS with parameters B_0 and B'_0 from ultrasonic experiments [8].

difference is illustrated in Fig. 3. At nominally 140 GPa, about the maximum pressure reached in the experiments, the difference between our calculated B'_0 value and that Ref. [7] translates to a pressure difference of about +11 GPa. This means that either repulsion is slightly overestimated in the calculations (independent of the exchange-correlation functional) or that the experimental data suffer from systematic errors, a combination of these effects not being ruled out. We will return to this issue below.

IV. OPTICAL PHONON FREQUENCY

A. Calculated phonon frequency versus volume

Figure 4 shows calculated F_{2g} phonon frequencies as a function of volume. At a given volume, the frequencies of all calculations are quite consistent with each other. The frequencies are too low by about 3% if compared to the experimental phonon frequency at ambient pressure. This small discrepancy does not originate from anharmonicity connected to the frozen-phonon displacement.

The volume dependence of phonon frequencies is usually characterized by the simple scaling law

$$\frac{\omega(V)}{\omega_0} = \left(\frac{V}{V_0} \right)^{-\gamma} = \left(\frac{\rho}{\rho_0} \right)^\gamma, \quad (6)$$

which assumes that the mode Grüneisen parameter $\gamma = -d \ln \omega / d \ln V$ is independent of volume. The frozen-phonon results indicate some volume dependence of γ ,

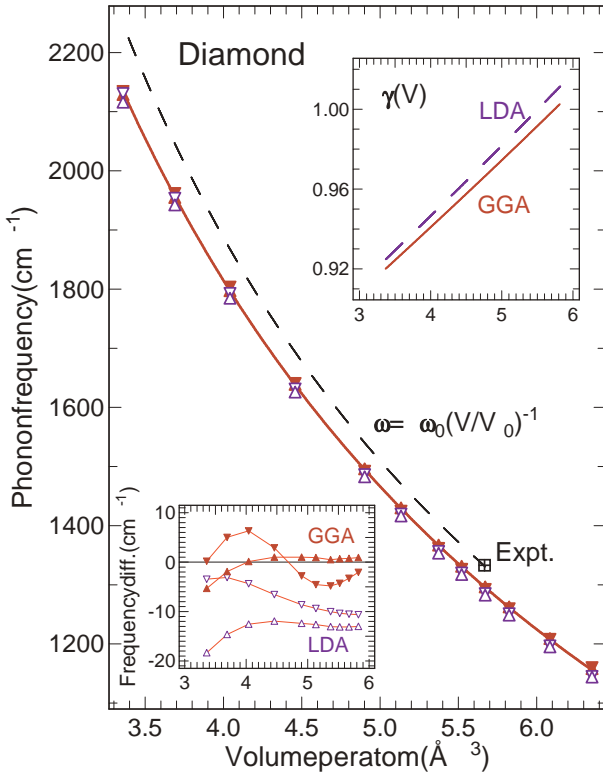


FIG. 4: Calculated zone-center optical phonon frequency of diamond as a function of atomic volume. The solid line guides through the combined GGA results. A Grüneisen relation Eq. 6 with parameters $\omega_0 = 1333 \text{ cm}^{-1}$ (experimental phonon frequency) and $\gamma_0 = 1$ is indicated for comparison (dashed line). Differences of individual calculated results with respect to the 'combined GGA' curve are shown in an inset. The second inset illustrates the calculated volume dependence of the mode Grüneisen parameter (for combined GGA and LDA results, respectively).

an observation which was also noted by Nielsen.²⁷ The expression

$$\frac{\Delta\omega(V)}{\omega_0} = \frac{\gamma_0}{\gamma'_0} \left[\left(\frac{V}{V_0} \right)^{-\gamma'_0} - 1 \right]. \quad (7)$$

with $\Delta\omega(V) = \omega(V) - \omega_0$ yields a slightly better match of our frozen-phonon results (3 cm^{-1} rms deviation or better for individual sets). Within standard deviations, the parameters γ_0 and γ'_0 for the combined GGA and LDA results are identical (see Table I). The upper inset to Fig. 4 illustrates the small volume dependence of the mode Grüneisen parameter resulting from $\gamma'_0 < 1$.

With $\rho/\rho_0 \approx \omega/\omega_0$ ($\gamma \approx 1$) it follows from Eq. 5 that the ratio of normalized bulk modulus to normalized phonon frequency is approximately linear in relative density and the slope is $B'_0 - 1$:

$$\frac{B}{B_0} \left(\frac{\omega}{\omega_0} \right)^{-1} \approx 1 + (B'_0 - 1) \frac{\Delta\rho}{\rho_0}. \quad (8)$$

This scaling between bulk modulus and optical phonon

frequency could come handy as a simple relation between an elastic and a dynamical property of diamond.

B. Calculated vs. experimental mode Grüneisen parameter

To compare the calculated phonon results with experimental data, we first consider the measured linear pressure coefficient of the phonon frequency. According to Schiferl *et al.*,²⁰ the 'best' experimental value in the literature, taken as the average of Refs. [4,15,19], should be $(d\omega/dP)_0 = 2.90 \pm 0.05 \text{ cm}^{-1}/\text{GPa}$ ($\gamma_0 \approx 0.96$). This value originates from experiments which employed the ruby pressure calibration with a linear coefficient $A = (dP/d\ln\lambda)_0 = 1905(10) \text{ GPa}$ for the R1 line wavelength (λ) shift near zero pressure as determined by Piermarini *et al.*⁷² Recent high-precision measurements of the ruby line shift up to 1 GPa⁷³ and a reinterpretation¹³ of R1 line shift data measured up to $\sim 20 \text{ GPa}$ ^{72,74} indicate that the parameter A is smaller ($A = 1820 \pm 30 \text{ GPa}$) compared to the previously accepted value. This revision leads to a corresponding increase of the phonon pressure coefficient. In this context it is helpful that the ratio of the diamond phonon frequency shift to ruby wavelength shift is explicitly given in Refs. [4] and [5]. The results, $7.94(10) \text{ cm}^{-1}/\text{nm}$ and $7.85(6) \text{ cm}^{-1}/\text{nm}$, agree quite well with each other. Taking the average value ($7.9(1) \text{ cm}^{-1}/\text{nm}$) in combination with $A = 1820(30) \text{ GPa}$, the corrected value from DAC experiments should be $(d\omega/dP)_0 = 3.0(1) \text{ cm}^{-1}/\text{GPa}$. Within experimental uncertainties, this linear pressure coefficient agrees with results obtained by methods which do not involve any ruby calibration,^{1,2,3} in particular that of Whalley *et al.*² With $B_0 = 444.8 \text{ GPa}$ the corresponding mode Grüneisen parameter becomes $\gamma_0 = 1.00(3)$, the error being mainly due to the uncertainty of the ruby coefficient A . We note the excellent agreement of the corrected experimental value for γ_0 with the results obtained within the LDA and GGA approximations (see Table I).

Occelli *et al.* report an *average* mode Grüneisen parameter of $\bar{\gamma} = 0.97$ for the range 0–140 GPa. It should be pointed out that their value of $\bar{\gamma}$ is independent of the pressure scale used in the experiments because the volume was measured directly. Taking into account the predicted volume dependence $\gamma(V)$ (see inset to Fig. 4), the calculations are fully consistent with the experimental volume dependence of the phonon frequency. This is no longer the case if we turn to the pressure dependence.

C. The pressure – phonon-frequency relationship

One can solve Eq. 7 for the relative volume, insert the corresponding expression into Eq. 2 (Eq. 4), and use the 'GGA' and 'LDA' parameters from Table I to obtain an analytical form for pressure as a function of phonon frequency. On the other hand, in the analysis

TABLE II: Calculated zone-center optical phonon properties of diamond. The parameters for the pressure versus frequency relation, Eq. 9, are given. Related experimental data are listed in the last two rows of the Table. Note that the linear pressure coefficient and the parameter b_0 are related by $(d\omega/dP)_0 = \omega_0/b_0 = \gamma_0\omega_0/B_0$.

Method or Source	ω_0 cm ⁻¹	b_0 GPa	η	$(d\omega/dP)_0$ cm ⁻¹ /GPa
All GGA	1290	429(6)	0.045(50)	3.00
All LDA	1322	460(3)	0.090(20)	2.87
Hanfland <i>et al.</i> ^a	1341	480	0.118	2.79
Nielsen ^b	1306	456	0.066	2.86
Experiment	1333	460	-	2.90(5) ^c
Experiment	1333	446	-	3.00(10) ^d

^aRef. [4].

^bRef. [27].

^cRefs. [20].

^dCorrected value based on revised linear pressure coefficient of the ruby R1 line shift.

of earlier phonon calculations,^{4,27} the $P(\omega)$ behavior was parametrized using the analog of a Birch expression⁶⁶

$$P(X) = \frac{3}{2}b_0(X^7 - X^5)[1 + \eta(1 - X^2)] \quad (9)$$

with $X = (\omega/\omega_0)^{1/3}$. Equation 9 (more or less an *ad hoc* choice in the earlier work) happens to yield excellent representations of the present calculated $P(\omega)$ results. To facilitate direct comparison with Refs. [4] and [27], the parameters b_0 and η are summarized in Table II. Note that for our calculated data η is the only adjustable parameter, because $b_0 = B_0/\gamma_0$.

Applicability of Eq. 4 in combination with $\gamma \approx 1$ implies a nearly quadratic dependence of pressure on change in phonon frequency. Thus, we compare calculated and experimental results in terms of reduced coordinates $P/\Delta\omega$ and $\Delta\omega$, cf. Fig. 5. Most of the calculated results represented in Fig. 5, i.e., the present ones within LDA and GGA and those of Refs. [4] and [27], agree very well with respect to the slope. This is of course reflected in the small scatter of the η values given in Table II. The average value from our calculations is

$$\eta = 0.068 \pm 0.03.$$

Inserting this value and the experimental data for ω_0 and $b_0 = \omega_0(dP/d\omega)_0$ (Table II) into Eq. 9 yields the $P(\omega)$ dependence consistent with experimental data near ambient pressure and with the nonlinear behavior predicted by the present calculations.

In the reduced coordinates of Fig. 5 the calculated $P(\omega)$ results of Wu and Xu⁴¹ do not agree well with those of other calculations. They use the quadratic function

$$\omega(P) = \omega_0 + a_1 P + a_2 P^2 \quad (10)$$

to fit their data. The choice of pressure as the independent variable in a quadratic expression is not appropriate

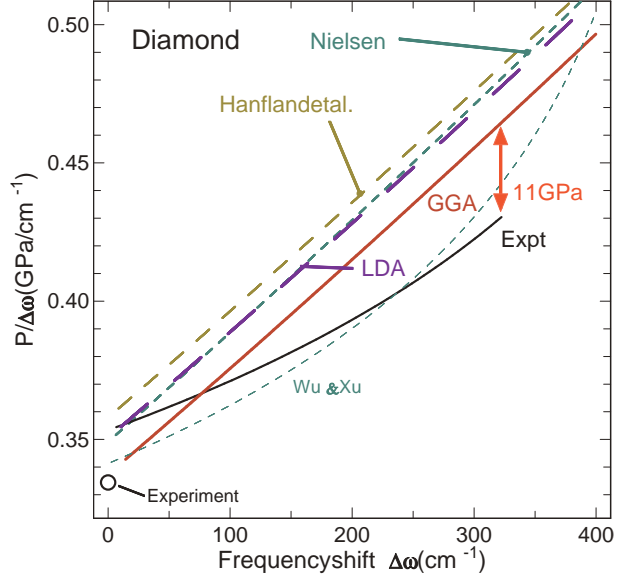


FIG. 5: Calculated pressure as a function of optical phonon frequency shift for diamond. A pressure range of about 200 GPa is covered. Pressure is divided by the frequency shift in order to illustrate the nearly quadratic dependence on frequency shift. In this representation the intercept at zero frequency shift corresponds to the inverse linear pressure coefficient $(d\omega/dP)^{-1}$. The open circle refers to the corrected experimental value. Besides the present LDA and GGA results, the figure shows the calculated results of Hanfland *et al.*,⁴ Nielsen,²⁷ and Wu & Xu.⁴¹ The experimental data of Occelli *et al.*⁷ are shown for comparison.

in view of Eq. 4 and $\gamma \approx 1$. It leads to parameter correlation which is the possible reason that their results exhibit curvature in Fig. 5.

Occelli *et al.*⁷ have measured the optical phonon frequency for pressures up to 140 GPa. They also give frequency as a quadratic function of pressure, i.e., $a_1 = 2.83 \text{ cm}^{-1}/\text{GPa}$ and $a_2 = -3.65 \times 10^{-3} \text{ cm}^{-1}/\text{GPa}^2$ in Eq. 10. The curvature of their data in Fig. 5 could again be related to the particular choice of the fitting function. The main observation, however, is that the average slope for the experimental data differs from the one predicted by theory. At the frequency corresponding to 140 GPa experimental pressure the pressure difference between calculations and experiment again amounts to about 11 GPa.

The sign and magnitude of this difference is very similar to that encountered when comparing experimental and calculated EOS results. Thus, in terms of pressure we find differences between calculated and experimental results which are about the same for different physical quantities considered. This hints to an explanation where the discrepancies are caused by the same systematic error(s).

V. REMARKS ON THE RUBY CALIBRATION

We consider the possibility that the discrepancy in the high pressure regime between experimental and calculated EOS and phonon frequency results for diamond are caused by some error in the experimental pressure scale, i.e. the calibration of the ruby R1 line shift according to Ref. [14].

Holzapfel¹³ recently proposed a revised ruby pressure scale, based on an analysis of published EOS data of selected elemental solids, including those of Ref. [7] for diamond. The revised ruby calibration was cast into a three-parameter analytical expression for pressure as a function of the R1 line wavelength. With the recommended parameter values¹³ and when restricted to about 200 GPa pressure (a range beyond the upper limit of most DAC studies), the revised calibration can be represented by a simple second-order polynomial in frequency shift $\Delta\nu$ of the R1 line. This is evident from Fig. 6 which shows plots of $(|\Delta\nu|/\nu_0)^{-1} \times P$ versus $|\Delta\nu|/\nu_0$ for Holzapfel's revised scale and for the 1978/1986 scales of Mao *et al.*^{14,75} We write the quadratic polynomial as⁷⁶

$$P(\Delta\nu) = A \frac{|\Delta\nu|}{\nu_0} \left[1 + \frac{B}{2} \frac{|\Delta\nu|}{\nu_0} \right]. \quad (11)$$

A linear regression for the 'Revised' line in Fig. 6 with $A = 1820$ GPa (fixed value as recommended in Ref. [13]) gives a slope parameter of $B=15.8$.

From the experimental $P(V)$ and $P(\omega)$ data of diamond⁷ one can recover the ruby line shift $\Delta\nu$ according to the ruby calibration¹⁴ used in the experimental work. Combining the experimental $V(\Delta\nu)$ and $\omega(\Delta\nu)$, respectively, with the calculated $P(V)$ and $P(\omega)$ relations reported here yields $P(\Delta\nu)$ as shown by the two solid lines in Fig. 6. These curves run more or less parallel to Holzapfel's revised calibration. Obviously, *both* the calculated $P(V)$ and $P(\omega)$ relations for diamond in combination with the experimental data of Ref. [7] support the proposed revision of the ruby pressure scale. It should be noted that the ruby calibration discussed by Aleksandrov *et al.*⁵ would be a little higher in pressure, but in the coordinates of Fig. 6 it exhibits a slope similar to that of the 'revised' line.

VI. CONCLUSIONS

We offer the following conclusions:

- (1) The results of the *first-principles* EOS and phonon frequency calculations for diamond reported here do not depend on the computational method, i.e., the choice of the crystal potential and basis sets in the PW, PAW, and APW+lo methods.
- (2) The calculated equilibrium values for volume (V_0) and bulk modulus (B_0) of diamond do depend on the exchange-correlation functional (LDA or GGA), a well-known fact in density functional theory. However, the

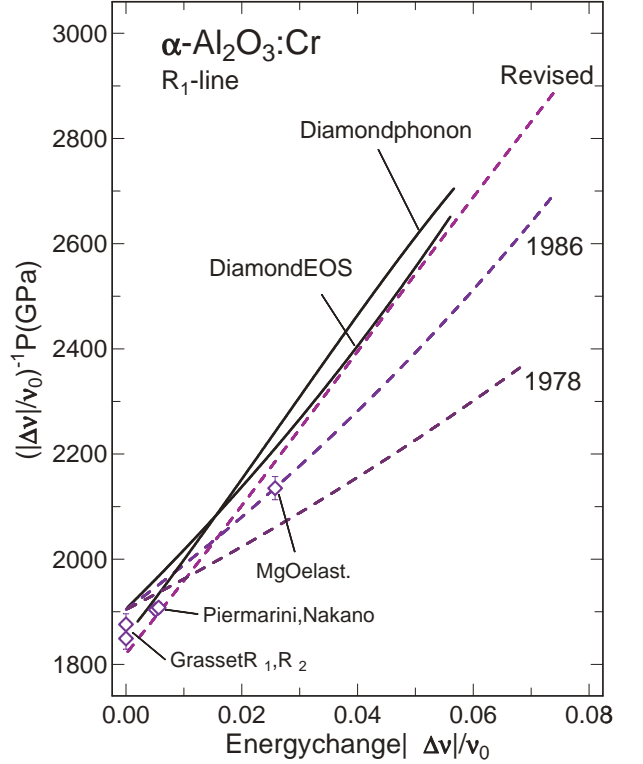


FIG. 6: Ruby pressure calibrations in reduced coordinates. Pressure is divided by energy change of the R₁ line and plotted as a function of the energy change. Dashed lines refer to the calibrations by Mao *et al.*^{14,75} (marked 1976 and 1986) and the revision proposed by Holzapfel.¹³ Lines marked 'diamond' refer to converted data of Occelli *et al.*⁷ combined with the calculated EOS and phonon frequency shift of diamond reported in the present work. The symbols near zero energy shift correspond to R₁ line pressure coefficients determined at low pressures.^{72,73,74} The symbol marked 'MgO' stands for the result of elasticity studies of MgO up to 55 GPa.⁷⁷

value of the pressure derivative of the bulk modulus [$B'_0=3.65(5)$] and the analytical form of the $P(V)$ relation are not affected within the volume range (40% compression) covered here. In other words, the calculated nonlinear component in the $P(V)$ behavior is independent of the method of calculation and the exchange-correlation approximation.

(3) The different theoretical methods and approximations also yield very similar results for the nonlinearity in the pressure versus phonon frequency relation $P(\omega)$.

(4) Both the calculated $P(V)$ and $P(\omega)$ relations exhibit a nonlinear behavior which is more pronounced than that observed in recent x-ray diffraction and Raman measurements of diamond up to 140 GPa.⁷ In terms of absolute pressure, the differences between theoretical and experimental results are essentially the same for the $P(V)$ and $P(\omega)$ behavior, of the order of 10 GPa at an experimental pressure of 140 GPa.

(5) Our calculated nonlinearity of $P(\omega)$ agrees well with that obtained in earlier *ab initio* phonon frequency

calculations for diamond under pressure.^{4,27} The work of Hanfland *et al.*⁴ indicated the need to reconsider the calibration of the ruby pressure scale used at that time.⁷⁵ The 'quasi-hydrostatic' (1986) ruby calibration¹⁴ reduced the discrepancy between theoretical predictions and experimental results. The remaining difference discussed here at least calls for some caution when experimental data measured above 50 GPa and based on the 1986 ruby pressure scale are compared to *ab initio* calculations or reduced shock wave data.

Acknowledgments

The authors thank P. Loubeyre and W. B. Holzapfel for making available preprints of Refs. [7] and [13], respectively. Part of the computer resources used in this work were provided by the Scientific Committee of IDRIS (Institut du Développement et des Ressources en Informatique Scientifique), Orsay (France).

* Permanent address: Laboratoire d'Optique des Solides, CNRS and Université Pierre and Marie Curie, T13-C80, 4 pl. Jussieu, F-75252 Paris - Cedex 05, France

† Corresponding author: E-mail k.syassen@fkf.mpg.de

¹ S. S. Mitra, O. Brafman, W. B. Daniels, and R. K. Crawford, Phys. Rev. **186**, 942 (1969).

² E. Whalley, A. Lavergne, and P. T. T. Wong, Rev. Sci. Instrum. **47**, 845 (1976).

³ M. H. Grimsditch, E. Anastassakis, and M. Cardona, Phys. Rev. B **18**, 901 (1978).

⁴ M. Hanfland, K. Syassen, S. Fahy, S. Louie, and M. Cohen, Phys. Rev. B **31**, 6896 (1985).

⁵ I. V. Aleksandrov, A. F. Goncharov, A. N. Zisman, and S. M. Stishov, Sov. Phys. JETP **66**, 384 (1987).

⁶ P. Gillet, G. Fiquet, I. Daniel, B. Reynard, and M. Hanfland, Phys. Rev. B **60**, 14660 (1999).

⁷ F. Occelli, P. Loubeyre, and R. LeToullec, Nature (2003), preprint of August 2002.

⁸ H. J. McSkimin and P. Andreatch, J. Appl. Phys. **43**, 2944 (1972).

⁹ M. H. Grimsditch and A. K. Ramdas, Phys. Rev. B **11**, 3139 (1975).

¹⁰ A. K. Ramdas, S. Rodriguez, M. Grimsditch, T. R. Anthony, and W. Banholzer, Phys. Rev. Lett. **71**, 189 (1993).

¹¹ R. Vogelgesang, A. K. Ramdas, S. Rodriguez, M. Grimsditch, and T. R. Anthony, Phys. Rev. B **54**, 3989 (1996).

¹² E. S. Zouboulis, M. Grimsditch, A. K. Ramdas, and S. Rodriguez, Phys. Rev. B **57**, 2889 (1998).

¹³ W. B. Holzapfel, J. Appl. Phys. **93**, 1813 (2003).

¹⁴ H. K. Mao, J. Xu, and P. M. Bell, J. Geophys. Res. **91**, 4673 (1986).

¹⁵ H. Boppert, J. Vanstraaten, and I. F. Silvera, Phys. Rev. B **32**, 1423 (1985).

¹⁶ A. F. Goncharov, I. N. Makarenko, and S. M. Stishov, JEPT Lett. **41**, 184 (1985).

¹⁷ I. Aleksandrov, A. F. Goncharov, and S. M. Stishov, JEPT Lett. **44**, 611 (1986).

¹⁸ A. Tardieu, F. Cansell, and J. P. Petitet, J. Appl. Phys. **68**, 3243 (1990).

¹⁹ M. Muinov, H. Kanda, and S. M. Stishov, Phys. Rev. B **50**, 13860 (1994).

²⁰ D. Schiferl, M. Nicol, J. M. Zaug, S. K. Sharma, T. F. Cooney, S. Y. Wang, T. R. Anthony, and J. F. Fleischer, J. Appl. Phys. **82**, 3256 (1997).

²¹ W. F. Sherman, J. Phys. C: Solid State Phys. **18**, L973 (1985).

²² A. Zunger and A. J. Freeman, Phys. Rev. B **15**, 5049 (1977).

²³ M. T. Yin and M. L. Cohen, Phys. Rev. Lett. **50**, 2006 (1983).

²⁴ J. R. Chelikowsky and S. G. Louie, Phys. Rev. B **29**, 3470 (1984).

²⁵ M. L. Cohen, Phys. Rev. B **32**, 7988 (1985).

²⁶ J. R. Chelikowsky, Phys. Rev. B **35**, 1174 (1987).

²⁷ O. H. Nielsen, Phys. Rev. B **34**, 5808 (1986).

²⁸ M. Cardona and N. Christensen, Solid State Commun. **58**, 421 (1986).

²⁹ S. Fahy and S. G. Louie, Phys. Rev. B **36**, 3373 (1987).

³⁰ S. Fahy, S. G. Louie, and M. L. Cohen, Phys. Rev. B **35**, 7623 (1987).

³¹ S. Fahy, K. J. Chang, S. G. Louie, and M. L. Cohen, Phys. Rev. B **35**, 5856 (1987).

³² S. Fahy, X. W. Wang, and S. G. Louie, Phys. Rev. Lett. **61**, 1631 (1988).

³³ C. Mailhot and A. K. McMahan, Phys. Rev. B **44**, 11578 (1991).

³⁴ P. E. Van Camp, V. E. Van Doren, and J. T. Devreese, Solid State Commun. **84**, 731 (1992).

³⁵ P. Pavone, K. Karch, O. Schütt, W. Windl, D. Strauch, P. Giannozzi, and S. Baroni, Phys. Rev. B **48**, 3156 (1993).

³⁶ M. Willatzen, M. Cardona, and N. Christensen, Phys. Rev. B **50**, 18054 (1994).

³⁷ S. J. Clark, G. J. Ackland, and J. Crain, Phys. Rev. B **52**, 15035 (1995).

³⁸ S. Scandolo, G. L. Chiarotti, and E. Tosatti, phys. stat. sol. (b) **198**, 447 (1996).

³⁹ S. Serra, G. Benedek, M. Facchinetto, and L. Miglio, Phys. Rev. B **57**, 5661 (1998).

⁴⁰ J. Xie, S. P. Chen, J. S. Tse, S. de Gironcoli, and S. Baroni, Phys. Rev. B **60**, 9444 (1999).

⁴¹ B. R. Wu and J. Xu, Phys. Rev. B **60**, 2964 (1999).

⁴² J. J. Zhao, S. Scandolo, J. Kohanoff, G. L. Chiarotti, and E. Tosatti, Appl. Phys. Lett. **75**, 487 (1999).

⁴³ P. Hohenberg and W. Kohn, Phys. Rev. **136**, B864 (1964).

⁴⁴ W. Kohn and L. J. Sham, Phys. Rev. **140**, A1133 (1965).

⁴⁵ J. P. Perdew and Y. Wang, Phys. Rev. B **45**, 13244 (1992).

⁴⁶ J. P. Perdew, S. Burke, and M. Ernzerhof, Phys. Rev. Lett. **77**, 3865 (1996).

⁴⁷ X. Gonze, J.-M. Beuken, R. Caracas, F. Detraux, M. Fuchs, G.-M. Rignanese, L. Sindic, M. Verstraete, G. Zerah, F. Jollet, M. Torrent, A. Roy, *et al.*, Computational Materials Science **25**, 478 (2002), URL <http://www.abinit.org>.

⁴⁸ S. Goedecker, SIAM J. Sci. Comp. **18**, 1605 (1997).

⁴⁹ M. Payne, M. Teter, D. Allan, T. Arias, and J. Joannopoulos, Rev. Mod. Phys. **64**, 1045 (1992).

⁵⁰ X. Gonze, Phys. Rev. B **54**, 4383 (1996).

⁵¹ P. Blacha, K. Schwarz, G. K. H. Madsen, D. Kvasnicka,

and J. Luitz, *WIEN2k, an augmented plane wave + local orbitals program for calculating crystal properties* (Karlheinz Schwarz, Techn. Universität Wien, Austria, 2001).

⁵² E. Sjöstedt, L. Nordström, and D. J. Singh, *Solid State Commun.* **114**, 15 (2000).

⁵³ G. K. H. Madsen, P. Blaha, K. Schwarz, E. Sjöstedt, and L. Nordström, *Phys. Rev. B* **64**, 195134 (2001).

⁵⁴ G. Kresse and J. Hafner, *Phys. Rev. B* **47**, R558 (1993); G. Kresse, Ph.D. Thesis, Technische Universität Wien (1993); G. Kresse and J. Furthmüller, *Comput. Mater. Sci.* **6**, 15 (1996); *Phys. Rev. B* **54**, 11169 (1996).

⁵⁵ G. Kresse and J. Joubert, *Phys. Rev. B* **59**, 1758 (1999).

⁵⁶ P. E. Blöchl, *Phys. Rev. B* **50**, 17953 (1994).

⁵⁷ C. Hartwigsen, S. Goedecker, and J. Hutter, *Phys. Rev. B* **58**, 3641 (1998).

⁵⁸ X. Gonze, private communication; see the pseudopotential entry at www.abinit.org for the parameters.

⁵⁹ O. H. Nielsen and R. M. Martin, *Phys. Rev. Lett.* **50**, 697 (1983).

⁶⁰ O. H. Nielsen and R. M. Martin, *Phys. Rev. B* **32**, 3780 (1985).

⁶¹ H. J. Monkhorst and J. D. Pack, *Phys. Rev. B* **13**, 5188 (1976).

⁶² O. Jepsen and O. K. Andersen, *Solid State Commun.* **9**, 1763 (1971).

⁶³ P. E. Blöchl, O. Jepsen, and O. K. Andersen, *Phys. Rev. B* **49**, 16223 (1994).

⁶⁴ T. Sato, K. Ohashi, T. Sudoh, K. Haruna, and H. Maeta, *Phys. Rev. B* **65**, 92102 (2002), the ambient-pressure lattice constants of pure diamond with natural isotopic composition are given as 3.56688 Å at 300 K and 3.566505 Å at 0 K.

⁶⁵ F. D. Murnaghan, *Proc. Nat. Acad. Sci. USA* **30**, 244 (1944).

⁶⁶ F. Birch, *J. Geophys. Res.* **83**, 1257 (1978).

⁶⁷ P. Vinet, J. Ferrante, J. R. Smith, and J. H. Rose, *J. Phys.: Cond. Matter* **19**, L467 (1986).

⁶⁸ W. B. Holzapfel, *Rep. Prog. Phys.* **59**, 29 (1996).

⁶⁹ F. D. Stacey, B. J. Brennan, and R. D. Irvine, *Geophys. Surv.* **4**, 189 (1981).

⁷⁰ S. Gaurav, B. S. Sharma, S. B. Sharma, and S. C. Upadhyaya, *Physica B* **322**, 328 (2002).

⁷¹ C. P. Herrero and R. Ramirez, *Phys. Rev. B* **63**, 24103 (2000).

⁷² G. J. Piermarini, S. Block, J. D. Barnett, and R. A. Forman, *J. Appl. Phys.* **46**, 2774 (1975).

⁷³ O. Grasset, *High Pressure Research* **21**, 139 (2001).

⁷⁴ K. Nakano, Y. Akahama, and Y. Ohishi, *Jpn. J. Appl. Phys.* **39** (3A), 1249 (1978).

⁷⁵ H. K. Mao, P. M. Bell, J. W. Shaner, and D. J. Steinberg, *J. Appl. Phys.* **49**, 3276 (1978).

⁷⁶ For practical purposes one may prefer to rewrite the $P(\nu)$ relation in terms of wavelength:

$$P(\lambda) = A \frac{\Delta\lambda}{\lambda} \left[1 + \frac{B}{2} \frac{\Delta\lambda}{\lambda} \right] .$$

Note that it is the wavelength at a given pressure which appears in the denominators.

⁷⁷ C.-S. Zha, H. Mao, and R. J. Hemley, *Proc. Nat. Acad. Sci. USA* **97**, 13494 (2000).